Molecular Crystals and Liquid Crystals
Publication details, including instructions for authors and subscription information:
http://www.tandfonline.com/loi/gmcl16

Interfacial and Temperature Gradient Effects On Thermal Conductivity of a Liqluid Crystal

Mukund N. Patharkar [a] , Varagur S. V. Rajan [a] & Jules J. C. Picot [a]
[a] Department of Chemical Engineering, Univesity of New Brunswick, Fredericton, N.B., Canada

To cite this article: Mukund N. Patharkar , Varagur S. V. Rajan & Jules J. C. Picot (1971): Interfacial and Temperature Gradient Effects On Thermal Conductivity of a Liqluid Crystal, Molecular Crystals and Liquid Crystals, 15:3, 225-237

To link to this article: http://dx.doi.org/10.1080/15421407108083238

Molecular Crystals and Liquid Crystals. 1971. Vol. 15, pp. 225–237

Printed in Great Britain

Interfacial and Temperature Gradient Effects on Thermal Conductivity of a Liquid Crystal

MUKUND N. PATHARKAR, VARAGUR S. V. RAJAN
and JULES J. C. PICOT

Department of Chemical Engineering
University of New Brunswick
Fredericton, N.B., Canada

Received January 4, 1971; *in revised form March* 19, 1971

Abstract—Thermal conductivity measurements were carried out on nematic *p*-azoxyanisole (commercial grade as well as purified PAA) with a steady state, cone and plate, variable gap, non-flow cell. Cell gaps were varied from 0.3175 cm to 0.0032 cm and temperature gradients were varied from 0.5 to 200 °C/cm. Effective thermal conductivity value increased progressively with decrease in gap and for the purified sample, it was about 12% higher at the lowest gap studied compared to the value at the largest gap studied and gradually decreased with increasing temperature gradient at each gap. A qualitative interpretation of the results is given with a discussion of the still unresolved problems.

1. Introduction

It is well known that the molecules of a nematic mesophase can be oriented by a number of influences such as proximity to an interface, shear, electric, and magnetic fields. Stewart *et al.*(8) reported that a temperature gradient also exerts an orienting influence for nematic *p*-azoxyanisole, an evidence which was subsequently questioned by Picot and Fredrickson(6) as well as by Fisher and Fredrickson.(3) Studies on molecular transport properties such as thermal conductivity(5,2); viscosity(7,2); and mass diffusivity(10) also show that nematic PAA exhibits anisotropic transport properties that are dependent upon the orienting influences. This paper reports on a study of the interfacial and temperature gradient effects on heat conduction in nematic PAA.

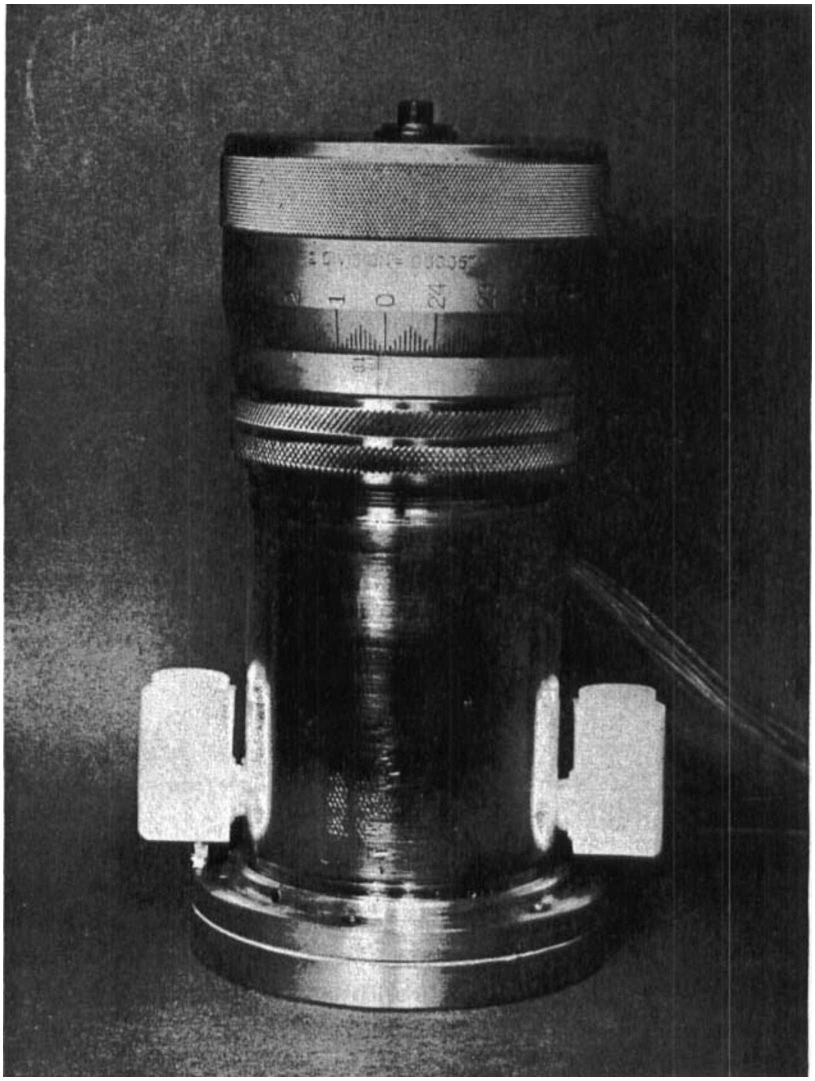

Figure 1. Photograph of thermal conductivity cell.

2. Experimental

The heat conduction studies were carried out in a non-flow, variable gap, steady state thermal conductivity cell shown in Fig. 1 with a schematic sectional diagram in Fig. 1(a). The working surface of the lower copper block *B* is conical in shape with an included angle of 179°. This geometry of cone and plate has a distinct advantage over two parallel plates in that it facilitates the setting of zero gap between the two plates by allowing the checking of the electrical

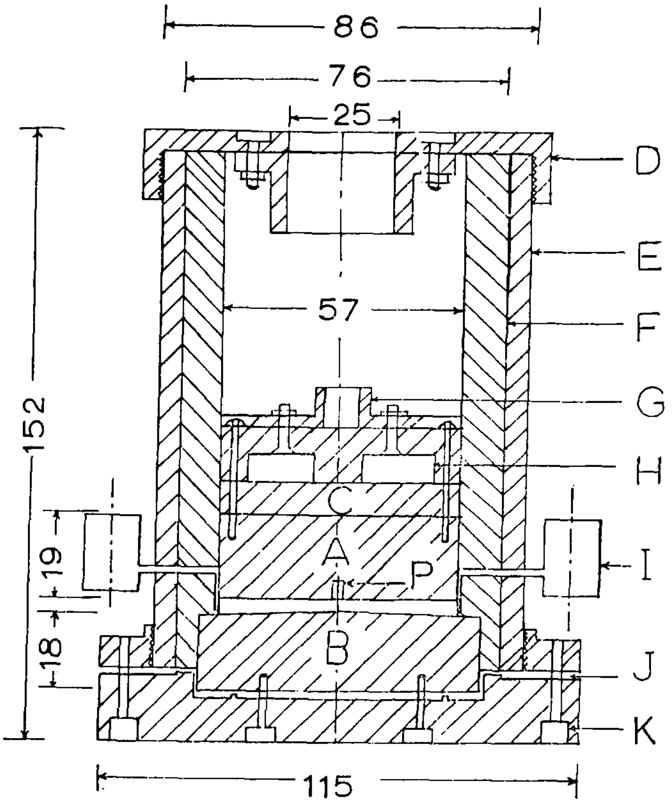

Figure 1(a). Schematic diagram of thermal conductivity cell. A—cell guard block with probe; B—cell lower conical block; C—cell heat distributor copper block; D—cell cap and micrometer reference base (stainless steel); E—brass outer sleeve; F—glass fibre impregnated teflon inner sleeve; G—micrometer spindle holder (stainless steel); H—cell heating coil enclosure (teflon); I—fluid filling and overflow reservoir (teflon); J—teflon base gasket; K—base plate; P—probe. All the dimensions are in millimeters.

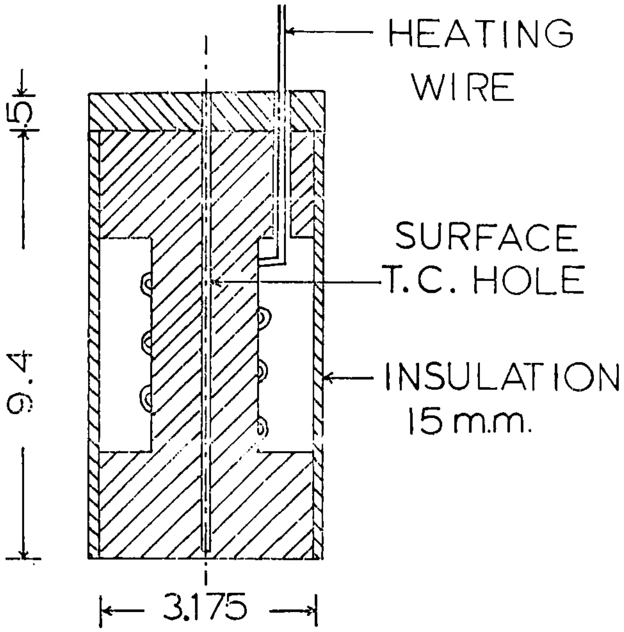

Figure 1(b). Schematic details of probe *P*. Heating wire consists of 20 turns of nichrome wire, non-inductively wound and electrically insulated from the probe. All the dimensions are in millimeters.

contact with the help of an external ohm-meter. The copper heating block *A* can be raised or lowered by means of a precision micrometer graduated to fifty millionths of an inch (0.00013 cm). Block *A* contains a heat flux probe (0.0792 sq cm in cross section) which includes a heating element and a surface thermocouple as shown in Fig. 1b. The cone tip was rounded off over an arc length approximately equal to the probe diameter. Surface thermocouples are located in blocks *A* and *B* at different radii, including one at the tip of the cone. The surfaces of blocks *A* (including the probe) and *B* were polished to a mirror finish, gold plated (to make it chemically resistant) and finally repolished. Filling tubes were attached to the cell and served as reservoirs for the excess fluid when the cell gap was decreased.

Thermal conductivity measurements were carried out with the cell placed in a constant temperature oven. A covered cylindrical copper sleeve was placed over the cylinder to provide for better temperature regulation to within ± 0.05 °C.

The operating procedure was to establish a steady state temperature difference between blocks A and B by adjusting the heating current to the block A heater, with the probe heater switched off. At steady state, the probe heater was switched on and adjusted to give zero temperature difference between block A surface and the probe surface at the new steady state. Under these conditions (block A acting as a thermal guard for the probe and being thermally insulated from it using Sauereisen 31 cement) the heat flux from the probe was completely directed into the fluid. The time required to reach the first steady state was one-half to one hour (after a change in setting of gap or heat input) and the time to achieve the second steady state was several minutes. At this steady state, the spatial and temporal (over several hours) temperature variation on the cell working surfaces was within ± 0.01 °C. The base oven temperature variation was maintained within ± 0.1 °C. The thermocouple e.m.f. was measured with a Leeds and Northrup guarded six dial potentiometer. Probe heat flux was calculated from the measurements on the electrical heat dissipation in the probe heater.

Cell calibration was carried out with a high viscosity polybutene oil (Petrofin 300, supplied by Petrofina of Canada Ltd.) at different gaps and temperature differences.

The p-azoxyanisol used was supplied by K & K Laboratories Inc., Plainview, N.Y. This commercial grade material (99% pure) was purified by four stages of recrystallization from ethanol. Transition temperatures were determined with a heated stage placed under a Reichert microscope and were as follows:

crystalline to nematic: 118.5 to 119.5 °C
nematic to isotropic: 135 °C.

The effective thermal conductivity is defined as follows:

$$k = k_{\text{eff}} = q\left|\frac{\Delta X}{\Delta T}\right|$$

where q = heat flux input at the probe surface

ΔX = distance between probe and tip of cone (assumed as two parallel plates)

ΔT = difference between probe temperature T_p and temperature of tip of cone T_c.

TABLE 1 Thermal Conductivity Data
(T_p in °C; q in cal/sq cm sec; $\Delta T/\Delta X$ in °C/cm and k_{eff} in cal/sec cm °C)

	Polybutene				Commercial PAA				Purified PAA			
ΔX	T_p	$q \cdot 10^4$	$\Delta T/\Delta X$	$k_{\mathrm{eff}} \cdot 10^4$	T_p	$q \cdot 10^4$	$\Delta T/\Delta X$	$k_{\mathrm{eff}} \cdot 10^4$	T_p	$q \cdot 10^4$	$\Delta T/\Delta X$	$k_{\mathrm{eff}} \cdot 10^4$
0.0175	125.26	2.31	0.952	2.43	126.22	2.91	0.970	3.00	125.31	3.00	0.936	3.22
	125.35	2.96	1.223	2.42	126.30	4.09	1.380	2.96	125.45	4.34	1.356	3.22
	125.45	4.08	1.688	2.42	126.35	4.89	1.630	3.00	125.48	4.63	1.443	3.22
	125.50	5.50	2.271	2.42	126.39	8.36	2.850	2.93	125.70	6.72	2.099	3.22
	—	—	—	—	—	—	—	—	125.73	7.94	2 470	3.22
0.1016	125.25	5.70	2.340	2.44	126.32	7.72	2.400	3.22	125.67	8.46	2.590	3.27
	125.44	9.90	4.085	2.42	126.19	8.26	2.600	3.18	125.60	9.75	3.010	3.25
	125.84	18.1	7.480	2.41	126.38	11.3	3.630	3.11	125.77	12.0	3.691	3.24
	—	—	—	—	126.15	14.7	4.780	3.07	126.01	14.9	4.560	3.25
	—	—	—	—	126.44	15.5	5.140	3.02	125.60	17.4	5.588	3.23
	—	—	—	—	126.58	21.3	7.054	3.02	125.60	19.0	6.070	3.14
	—	—	—	—	126.22	21.6	7.220	3.01	125.55	23.2	7.550	3.07
	—	—	—	—	—	—	—	—	125.67	26.4	8.200	3.23
0.0508	125.40	15.4	6.300	2.44	126.41	17.1	5.040	3.38	126.05	16.2	4.920	3.29
	125.73	20.4	8.290	2.46	126.40	17.3	5.120	3.38	125.90	17.1	5.195	3.29
	125.50	21.9	8.990	2.44	126.32	18.5	5.520	3.35	125.66	20.4	6.222	3.27
	125.91	31.3	12.82	2.44	126.08	20.0	6.000	3.34	126.15	26.2	8.010	3.27
	—	—	—	—	126.52	27.4	8.460	3.23	125.38	28.2	8.695	3.24
	—	—	—	—	126.15	29.9	9.340	3.20	125.92	31.6	9.790	3.22
	—	—	—	—	126.60	33.0	10.39	3.18	125.90	35.3	11.05	3.20
	—	—	—	—	126.65	38.3	12.23	3.13	125.85	37.9	12.15	3.12
	—	—	—	—	126.05	51.8	16.79	3.09	125.32	41.9	12.88	3.24
	—	—	—	—	—	—	—	—	125.78	43.1	14.22	3.04
0.0254	125.56	24.8	10.17	2.43	126.25	25.4	7.070	3.59	126.08	25.1	7.555	3.32
	125.97	44.7	18.37	2.43	126.51	26.8	7.300	3.66	125.98	38.8	11.81	3.28
	125.61	52.0	21.30	2.44	126.35	43.6	11.81	3.69	125.92	42.0	12.86	3.27
	125.72	61.8	25.37	2.44	126.37	48.3	13.82	3.49	125.81	48.8	14.98	3.25
	—	—	—	—	126.34	56.7	16.84	3.37	125.76	52.3	16.18	3.23
	—	—	—	—	126.48	69.1	20.89	3.31	125.72	53.9	16.67	3.23
	—	—	—	—	126.52	77.2	24.06	3.21	125.65	63.5	19.68	3.22

	—	—	—	—	126.28	89.7	28.06	3.20	125.49	67.4	20.34	3.21
	—	—	—	—	126.22	90.0	28.43	3.17	125.36	73.9	23.14	3.21
	—	—	—	—	—	—	—	—	125.23	83.2	26.03	3.21
	—	—	—	—	—	—	—	—	125.21	89.6	28.06	3.19
	—	—	—	—	—	—	—	—	125.23	94.5	29.57	3.20
0.0127	125.27	37.7	15.62	2.41	126.45	63.0	16.45	3.83	125.65	37.6	11.05	3.40
	125.36	94.3	39.02	2.42	126.32	66.7	17.41	3.83	125.61	44.7	13.17	3.40
	125.62	133.0	55.29	2.41	126.35	76.3	20.30	3.76	125.59	56.7	16.62	3.41
	—	—	—	—	126.20	95.0	25.37	3.74	125.43	81.6	24.23	3.37
	—	—	—	—	126.25	101.0	27.52	3.67	125.51	93.5	24.54	3.40
	—	—	—	—	126.65	112.0	31.89	3.50	125.37	115.0	34.12	3.37
	—	—	—	—	126.41	156.0	46.85	3.34	126.16	115.0	34.21	3.36
	—	—	—	—	126.38	164.0	49.78	3.29	125.75	123.0	37.01	3.33
	—	—	—	—	126.22	174.0	55.12	3.16	125.85	154.0	46.67	3.29
	—	—	—	—	126.53	201.0	63.43	3.17	125.83	145.0	47.68	3.28
	—	—	—	—	—	—	—	—	125.60	172.0	49.43	3.29
	—	—	—	—	—	—	—	—	125.65	171.0	52.93	3.23
0.0064	125.76	11.6	48.38	2.40	126.25	109.0	23.80	4.57	125.58	89.5	25.68	3.48
	125.69	18.0	73.75	2.44	126.45	107.0	23.97	4.47	126.17	96.5	27.69	3.48
	126.10	24.2	100.8	2.40	126.43	169.0	39.02	4.32	126.04	111.0	31.15	3.47
	—	—	—	—	126.35	175.0	41.38	4.24	125.84	120.0	34.82	3.43
	—	—	—	—	126.48	270.0	65.70	4.10	126.08	130.0	37.79	3.44
	—	—	—	—	126.48	281.0	68.94	4.07	125.57	166.0	49.86	3.43
	—	—	—	—	125.55	306.0	79.79	3.84	125.61	196.0	58.62	3.35
	—	—	—	—	126.55	328.0	84.95	3.86	125.41	212.0	62.82	3.37
	—	—	—	—	126.56	347.0	91.43	3.79	125.44	214.0	65.70	3.26
	—	—	—	—	126.61	369.0	102.5	3.60	125.31	243.0	75.15	3.24
	—	—	—	—	126.65	390.0	109.5	3.56	125.22	267.0	83.10	3.31
	—	—	—	—	126.60	422.0	117.8	3.58	125.18	307.0	96.24	3.28
	—	—	—	—	126.65	434.0	122.1	3.56	125.21	307.0	97.99	3.13
	—	—	—	—	—	—	—	—	125.35	342.0	114.6	2.98
0.0032	—	—	—	—	—	—	—	—	126.27	317.0	88.35	3.59
	—	—	—	—	—	—	—	—	125.97	383.0	108.5	3.53
	—	—	—	—	—	—	—	—	126.03	408.0	117.0	3.48
	—	—	—	—	—	—	—	—	125.58	560.0	164.5	3.34
	—	—	—	—	—	—	—	—	125.53	614.0	182.1	3.37
	—	—	—	—	—	—	—	—	126.14	810.0	246.7	3.28

The subscripts a, t, ran, are used to indicate the axial, transverse and random orientation thermal conductivity values of the ellipsoidal swarms of nematic PAA.

3. Discussion of Results

The accompanying table of data (Table 1) shows results for polybutene oil in the temperature range of about 125–126 °C and similar results were obtained for PAA for all gaps in the temperature range of about 140–141 °C when it is in the isotropic liquid state. From these results, it can be seen that there is no systematic change in the thermal conductivity value with changes in gap size and temperature difference which indicates that the cell design and operation are such that the results are free of experimental artifact for these isotropic liquids. These results validate the parallel plate assumption in the definition of k_{eff}.

The statistical average value of k_{eff} for polybutene oil was found to be 2.43×10^{-4} cal/cm sec °C which agrees very well with the value 2.47×10^{-4} cal/cm sec °C reported by the supplier. Similarly the average k_{eff} for isotropic PAA was 3.75×10^{-4} cal/cm sec °C which compares with a value of 3.75×10^{-4} cal/cm sec °C given by McCoy and Kowalczyk.(4) The greatest deviation from the average was 1.2% for polybutene and less than 1% for isotropic PAA.

Figures 2 and 3 show the thermal conductivity results for nematic PAA (commercial grade and purified PAA respectively). The experimental data are plotted as k/k_{ran} against the temperature gradient for different gaps. The temperature gradient is an overall value and is equivalent to $|\Delta T/\Delta X|$. As can be seen from Figs. 2 and 3, k/k_{ran} is dependent both upon the gap and the temperature gradient.

Picot and Fredrickson(6) reported a thermal conductivity value of 3.2×10^{-4} cal/cm sec °C for randomly oriented nematic PAA. This value compares with 3.22×10^{-4} cal/cm sec °C at 123 °C as reported by Fisher and Fredrickson(3) and 3.28×10^{-4} cal/cm sec °C as reported by McCoy and Kowalczyk.(4) Our lowest value of thermal conductivity of 3.22×10^{-4} cal/cm sec °C at 0.3175 cm gap (where for purified PAA, the interfacial effects appear to be negligible) agrees well with the previously reported values and this is used as k_{ran}.

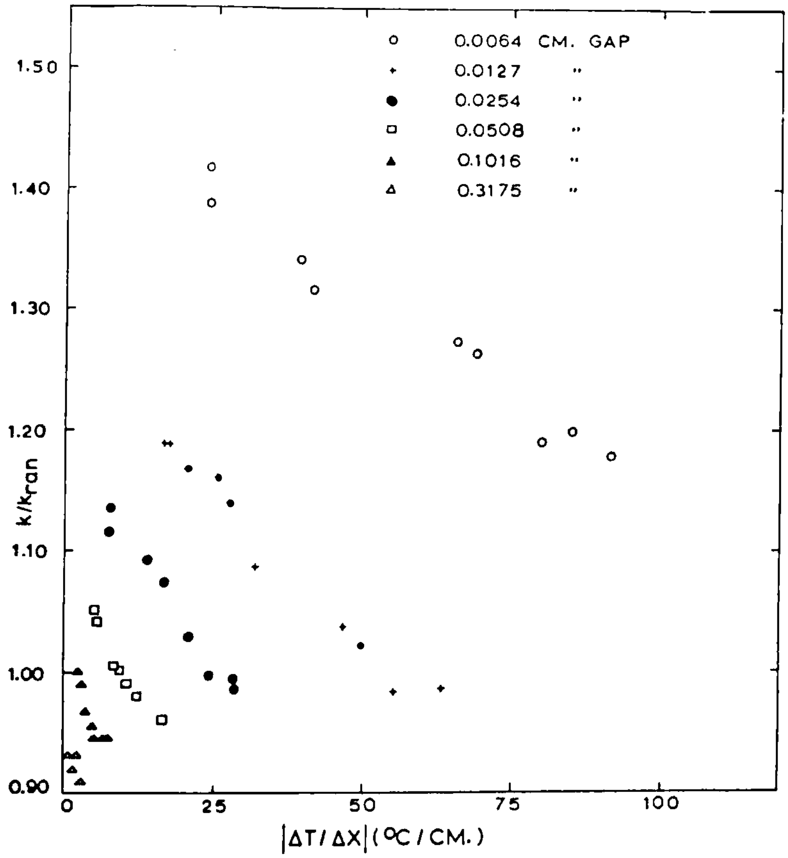

Figure 2. Reduced thermal conductivity of *p*-azoxyanisole (commercial grade) as a function of gap and temperature gradient. $k_{\text{ran}} = 3.22 \times 10^{-4}$ cal/cm sec °C.

There are two important aspects of the results on Figs. 2 and 3. First, an interfacial effect is evident. For the purified PAA (Fig. 3), the largest value of k_{eff} was 3.59×10^{-4} cal/cm sec °C for 0.0032 cm gap. For the commercial sample the value of k_{eff} ranges from 2.93×10^{-4} cal/cm sec °C for 0.3175 cm gap to 4.57×10^{-4} cal/cm sec °C for 0.0064 cm gap. The latter results agree well with those reported by Picot and Fredrickson[6] who reported 41% higher thermal conductivity in the highly oriented surface layer than in the bulk phase for a commercial sample. The results on the purified

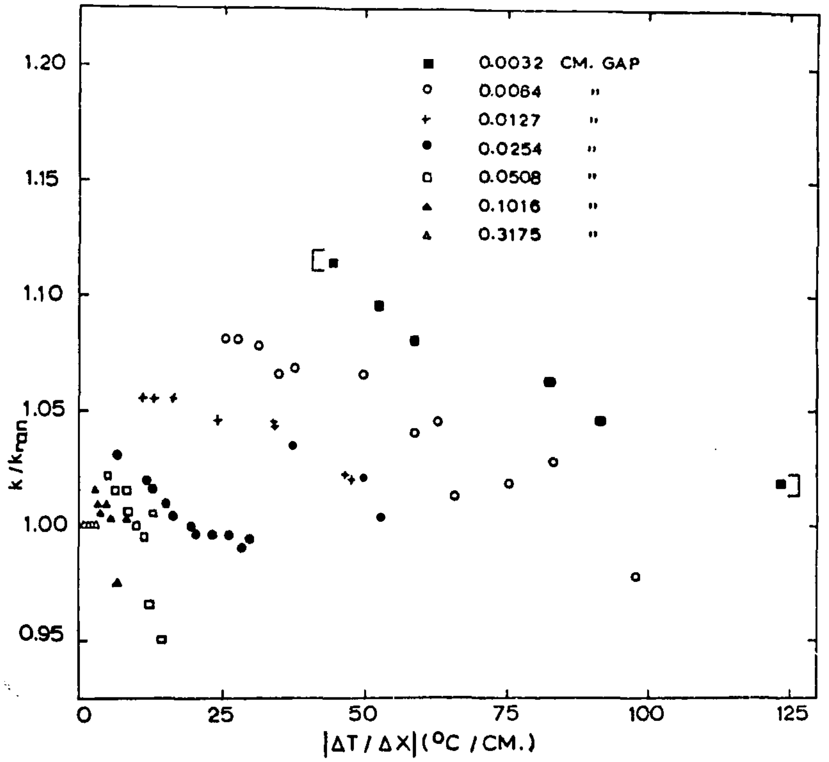

Figure 3. Reduced thermal conductivity of purified *p*-azoxyanisole as a function of gap and temperature gradient. (Note: Abscissa for 0.0032 cm gap reads from 0 to 250). $k_{ran} = 3.22 \times 10^{-4}$ cal/cm sec °C.

PAA agree reasonably well with the results of Fisher and Fredrickson[3] at 123 °C where a fully oriented bulk phase at very high shear rate showed a 5.54% higher thermal conductivity than a randomly oriented bulk phase at zero shear rate. The shear field is claimed by the aforementioned authors to produce complete parallel orientation of the nematic swarms. Therefore, $k_t > k_a$. Assuming this to be true, the present study indicates that ellipsoidal nematic swarms of PAA are oriented with their long axes parallel to the cell surface with a gradual decay in degree of uniform orientation with distance away from the interface. When the two cell surfaces are very close together, the nematic liquid in the narrow gap could be completely oriented in a direction parallel to the surface. Yun[11] has conducted similar studies on nematic *p*-*n*-decyloxybenzoic acid under the orienting influence of magnetic field, and found that swarm to surface orientation was perpendicular.

A second apparent thermal conductivity effect (from Figs. 2 and 3) is the decrease in thermal conductivity with increase in the temperature gradient. There could be several reasons for this:

(1) The increase in the bulk temperature of the sample when temperature gradient is increased will reduce the thermal conductivity. For the case of 0.0032 cm gap, the decrease in thermal conductivity (Fig. 3) is of the order of 9%, whereas McCoy and Kowalczyk's⁽⁴⁾ results indicate that the reduction due to a temperature increase of 0.4 °C would be less than 1%. This hypothesis is therefore discarded.

(2) The phenomenon of temperature gradient induced orientation has been discussed in the literature by Stewart et al.⁽⁸⁾, by Picot and Fredrickson,⁽⁶⁾ and by Fisher and Fredrickson.⁽³⁾ The first of these papers reports (from X-ray studies) that a temperature gradient (1 to 2 °C/cm) produces orientation of the nematic swarms of PAA. In the second paper, the apparent thermal conductivity in the surface zone of the hot-wire probe was not altered by a two-fold variation in the impressed heat flux. In the latter paper, for the experiments in a concentric cylinder annular flow cell, the effective thermal conductivity was not altered when the temperature gradient in the gap was varied from about 12 to 36 °C/cm. The results of Fisher and Fredrickson also indicate that in the presence of a shear field, there is a negligible influence of temperature gradient on orientation. The results of Stewart et al. indicate strong orientation effects in a non-flow cell (assuming that natural convection was satisfactorily eliminated) induced by a temperature gradient. The experimental evidence that $k_t > k_a$ for the nematic swarms of PAA indicates that the effect of temperature gradient is to orient the swarms in a direction perpendicular to that of the orienting influence of the interface. A parallel orientation of the swarms at the interface is assumed as explained before. This tendency of the temperature gradient explains the reduction in the k_{eff} values with increase in the temperature gradient.

Though the effect of temperature gradient at large gaps in our results as well as those of the past workers is inconclusive, it is our general conclusion that the temperature gradient effect is strongly coupled with the interfacial orienting influence in the transport phenomena in liquid crystals.

There is also evidence in our results presently reported that the orienting influence of temperature gradient is of considerably different magnitude for purified and commercial samples of PAA.

4. Concluding Remarks

The above evidence of temperature gradient induced orientation requires that the external field flux term **F** in the equation of change given below for the anisotropy tensor introduced by Sullivan⁽⁹⁾ should include the effect of temperature gradient also:

$$\frac{D\mathbf{A}}{Dt} = -6D_r\mathbf{A} + \lambda\Delta^2\mathbf{A} + \mathbf{F}.$$

In this expression the anisotropy tensor **A** is given by:

$$\mathbf{A} = \langle \underline{N}\underline{N} \rangle - 1/3\mathbf{I}.$$

$\underline{N}$ is the unit vector directed along the long axis of the swarm, and the expression $\langle \underline{N}\underline{N} \rangle$ is the local ensemble average value of the dyadic product $\underline{N}\underline{N}$ and **I** is the identity tensor. D/Dt is the convected time derivative; D_r is the rotational diffusion coefficient; λ is a particle interaction term; and the term **F** is represented as follows:

$$\mathbf{F} = f(\nabla\underline{v}, \underline{H}, \nabla\underline{T}, \overset{*}{\mathbf{e}})$$

The form of **F** based on $\nabla\underline{v}$ (electric field strength), $\underline{H}$ (magnetic field strength), and $\overset{*}{\mathbf{e}}$ (rate of strain tensor) is discussed by Fisher⁽²⁾ and by Sullivan.⁽⁹⁾ It is not obvious at this stage, how the dependency of heat flux on $\nabla\underline{T}$ should be expressed, but the results indicate a non-linear relationship between the heat flux vector and $\nabla\underline{T}$.

For transversely isotropic ellipsoidal particles in which the transverse and axial thermal conductivities are different, the following relation holds as shown by Fisher⁽²⁾:

$$k_{\text{ran}} = \tfrac{1}{3}(k_a + 2k_t).$$

In the above discussion, the maximum thermal conductivity for the purified sample was 3.59×10^{-4} cal/cm sec °C, and it was 4.57×10^{-4} cal/cm sec °C for the commercial sample, and this is for a high degree of orientation of swarms perpendicular to the direction of temperature gradient. This value can be assumed to be close to the value of k_t. The value of k_a computed analytically by Fisher(2) is 2.82×10^{-4} cal/cm sec °C. The preceding relation between the thermal conductivities then gives a value of k_a of 2.48×10^{-4} cal/cm sec °C for the purified PAA sample and a k_a value of 0.52×10^{-4} cal/cm sec °C is obtained for the commercial grade sample using our value of k_t.

Carr(1) has pointed out that impurities in the sample as well as the surface play an important role in the orientation of liquid crystals. It is not clear at this stage, how the effect of impurities could be explained in terms of orientation mechanism. Further investigation is necessary to give a better understanding of the transport phenomena in liquid crystals.

REFERENCES

1. Carr. E. F. in " Ordered Fluids and Liquid Crystals " Ed. by Gould, R. F., *Advances in Chemistry Series No. 63*, American Chemical Society, Washington, D.C., 76 (1967).
2. Fisher, J., " Transport Phenomena in Liquid Crystals ", Ph.D. Thesis, University of Minnesota (1969).
3. Fisher, J. and Fredrickson, A. G., *Mol. Cryst. and Liq. Cryst.* **6**, 255 (1969).
4. McCoy, J. B. and Kowalczyk, L. S., *Chem. Eng. Prog. Symp. Series No. 30* **56**, 11 (1960).
5. Picot, J. J. C., " Temperature History and Fluid–Solid Interface Effects on Heat Conduction in Certain Liquids ", Ph.D. Thesis, University of Minnesota (1966).
6. Picot, J. J. C. and Fredrickson, A. G., *I and EC Fundamentals* **1**, 84 (1968).
7. Porter, R. S. and Johnson, J. F. in *Rheology*, Ed. by Eirich, F. R., Academic Press, New York, 317 (1967).
8. Stewart, G. W., Holand, D. O. and Reynolds, L. M., *Phys. Rev.* **58**, 174 (1940).
9. Sullivan, J. T., " Transport Phenomena in Liquid Crystals ", Ph.D. Thesis, University of Minnesota, 1966.
10. Svedberg, T., *Kolloid Z.* **22**, 68 (1918).
11. Yun, C. K., " Transport Phenomena in Liquid Crystals ", Ph.D. Thesis, University of Minnesota, 1970.